CHEMISTRY
AN ASIAN JOURNAL

DOI: 10.1002/asia.200600169

Crystalline Vanadium Pentoxide with Hierarchical Mesopores and Its Capacitive Behavior

Hongtao Liu,[a] Ping He,[b] Zhiying Li,[a] Danzi Sun,[a] Haiping Huang,[a] Jinghong Li,[a, c] and Guoyi Zhu*[a]

Abstract: Crystalline vanadium pentoxide with hierarchical mesopores was synthesized by using a CTAB/BMIC cotemplate (CTAB = cetyltrimethylammonium bromide, BMIC = 1-butyl-3-methylimidazolium chloride). The material was fully characterized by SEM, TEM, N_2 adsorption–desorption, XRD, XPS, and CV methods. By elaborate adjustment of the template proportions, the distribution and size of the hierarchical pores were tuned successfully. CTAB cationic surfactant contributed more to the larger mesopores, whereas BMIC ionic liquid was beneficial in forming the smaller nanopores. The vanadium-containing anions combined with CTA^+ micelles and BMI^+ rings through electrostatic interactions. The CTA^+–$O(VO)O^-$–BMI^+ entities built up an orderly array, which finally formed the hierarchical mesoporous framework during thermal treatment. The mesoporous vanadium pentoxide directed by the cotemplate of CTAB/BMIC = 1:1 showed many orderly crystalline structures and demonstrated a large capacitance (225 $F g^{-1}$); it is thus a promising material for electrochemical capacitors. Two alternative solutions to the disappearance of capacitance due to insertion of K^+ are proposed in view of possible future applications.

Keywords: capacitance · ionic liquids · mesoporous materials · template synthesis · vanadium

Introduction

Since the first mesoporous solid MCM-41, which has a regular, ordered pore arrangement and a very narrow pore-size distribution, was discovered in 1992,[1] mesoporous materials have attracted much attention in synthesis, characterization, mechanism research, and morphology control. Owing to their enhanced electronic, magnetic, optical, and catalytic properties, these materials may be widely applied in many trades and professions.[2–12] To enlarge the pore size to greater than 2 nm, the structure-directing templates of block copolymer surfactants and swelling agents were universally employed for most mesoporous materials.[13–18] Recently, highly ordered supermicroporous materials with pore sizes of less than 2 nm were prepared by nanocasting techniques, which bridged the gap between microporous and mesoporous materials.[19,20] However, little effort has been devoted to the construction of hierarchical mesoporous materials in which the smaller pores are distributed within the corresponding larger ones.[21] Crystalline ceria with a bimodal pore system was reported more recently by Smarsly and coworkers,[21] who adopted a suitable block copolymer with the combination of an ionic surfactant as a cotemplate to generate the hierarchical porous framework. In general, such hierarchical porous materials are more promising than monomodal mesoporous materials in practical applications.[22]

Mesoporous metal oxides, as the most important functional semiconductor materials, have always been widely investigated.[23–29] The fact that vanadium pentoxide acts as an advanced intercalation host material for Li^+, K^+, Na^+, Mg^{2+}, Ca^{2+}, and so on[30–34] attracted great interest in the fields of electrochemistry and materials science. Vanadium pentoxide has also been used as a highly efficient catalyst for asymmetrical oxidation[35] and removal of pollution gases.[36] Howev-

[a] H. Liu, Z. Li, D. Sun, H. Huang, J. Li, G. Zhu
State Key Laboratory of Electroanalytical Chemistry
Changchun Institute of Applied Chemistry
Chinese Academy of Sciences
Changchun 130022 (China)
and Graduate School of the Chinese Academy of Sciences
Beijing 100039 (China)
Fax: (+86) 431-5262069
E-mail: zhuguoyi@ciac.jl.cn

[b] P. He
College of Material Science and Engineering
Southwest University of Science and Technology
Mianyang 621010 (China)

[c] J. Li
Department of Chemistry, Tsinghua University
Beijing 100084 (China)

er, so far only monomodel mesoporous vanadium pentoxide has been synthesized with the aid of surfactants.[37,38] Hierarchical mesoporous vanadium pentoxide with orderly pores distributed within the material has not yet been found. A main problem in the preparation of hierarchical mesoporous crystalline structures is related to the collapse of the pores due to stress arising from crystallization of the matrix. Therefore, a general methodology would be the use of appropriate amphiphilic templates with different sizes, and the two surfactants have to be compatible with respect to their cohesion energies to avoid phase separation.

Ionic liquids (ILs) have recently received much attraction in many fields of chemistry and industry, owing to their potential as a green recyclable alternative to traditional organic solvents.[39] They have a long liquidus, in some cases in excess of 400 °C. Their highly favorable properties, such as negligible vapor pressure, wide electrochemical window, high ionic conductivity, and thermal stability, make ILs effective in catalysis,[40–42] electrochemistry,[43–47] liquid–liquid extraction,[48–50] and organic liquid-phase reactions.[51–55] Most of the room-temperature ILs (RTILs) investigated consist of organic 1-alkyl-3-methylimidazolium cations and organic or inorganic anions. The positively charged imidazolium rings play crucial roles in the formation of the wormhole framework of mesoporous silica.[56] In view of the structure-directing role of the rings, the imidazolium-based ILs may be suitable candidates as soft templates for the synthesis of mesoporous materials.

Herein, we used 1-butyl-3-methylimidazolium chloride (BMIC) IL and cetyltrimethylammonium bromide (CTAB) cationic surfactant as a cotemplate to synthesize mesoporous vanadium pentoxide. BMIC with structure-directing rings and CTAB with orderly cationic micelles can model hierarchical multiporous morphologies. Furthermore, BMIC and CTAB are very compatible with each other; they avoid the phase separation and have a synergetic effect on the formation of the hierarchical porous framework of vanadium pentoxide. By elaborate adjustment of the ratios of the two template reagents, the distribution and size of the hierarchical pores of the material can be tuned. The hierarchical porous crystalline vanadium pentoxide with regard to its very large surface area is expected to act as a good capacitive material.

Results and Discussion

Figure 1 shows the surface structures and morphologies of porous vanadium pentoxides synthesized by using two typical ratios of template reagents. It is evident from Figure 1a that most flakes and clumps of 30–40 nm were agglomerated when the structure-directing template contained an absolute excess of cationic surfactant CTAB (molar ratio CTAB/BMIC = 5:1). When the IL was increased such that CTAB/BMIC = 1:1 (Figure 1c), the products obtained were much smaller and finer. The particles became less conglomerated into clusters and much rounder compared to those obtained

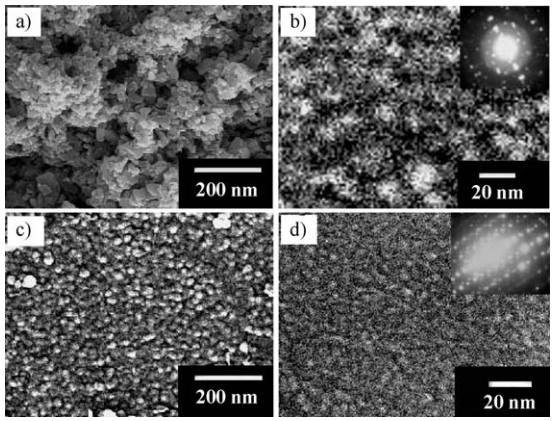

Figure 1. a) and c) Scanning electron microscopy (SEM) and b) and d) transmission electron microscopy (TEM) images of the crystalline vanadium pentoxides formed by using CTAB/BMIC templates with the molar ratio of a) and b) 5:1 and c) and d) 1:1. The corresponding ED patterns are shown in the insets of b) and d).

with insufficient BMIC IL. The excess CTAB with the twisted alkyl-chain tails easily modeled irregular nanoscale cavities (Figure 1b). The crystalline pattern (Figure 1b, inset) was indexed as orthorhombic V_2O_5 along the [001] and [110] directions. The CTAB/BMIC cotemplate samples produced hierarchical porous structures in which mesopores of roughly 6–10 nm were formed between uniformly and closely distributed particles; meanwhile, numerous far-smaller pits of less than 2 nm were located on the walls of these round particles (Figure 1d). This indicates that the cotemplate with a suitable proportion of IL is advantageous for modeling orderly hierarchical pores within materials. The hierarchical porous V_2O_5 material has an orthorhombic crystalline pattern (Figure 1d, inset) along the [001] growth direction. Previous XRD data also confirmed that sol-gel-derived films have polycrystalline structures with preferential orientation along the [001] axis.[57] These results imply that the introduction of the IL has an important effect on the crystalline growth orientation and therefore, to a large extent, models the size and morphology of the material formed.

Figure 2 shows the N_2 adsorption–desorption isotherms and the corresponding pore-size distributions (inset) of the synthesized crystalline vanadium pentoxides. The behavior of the adsorption–desorption isotherms of porous materials are dependent not only on pore size but also on pore morphology. The narrow hysteresis loops that appeared at different relative pressures are characteristic of hierarchical pores. The increase in adsorbed volume at high relative pressure is a direct indication of the presence of the secondary large pores. The vanadium pentoxides from the CTAB leading template (with insufficient BMIC IL) have a Brunauer–Emmett–Teller (BET) surface area $255\ m^2 g^{-1}$ with two broad ranges of pore sizes, whereas the products of the CTAB/BMIC cotemplate, with a BET surface area of $262\ m^2 g^{-1}$, present much narrower hierarchical pore distributions centered at 1.8 and 8.7 nm (Figure 2, inset). The narrow pore-size ranges arise from the equivalent amount

CHEMISTRY
AN ASIAN JOURNAL

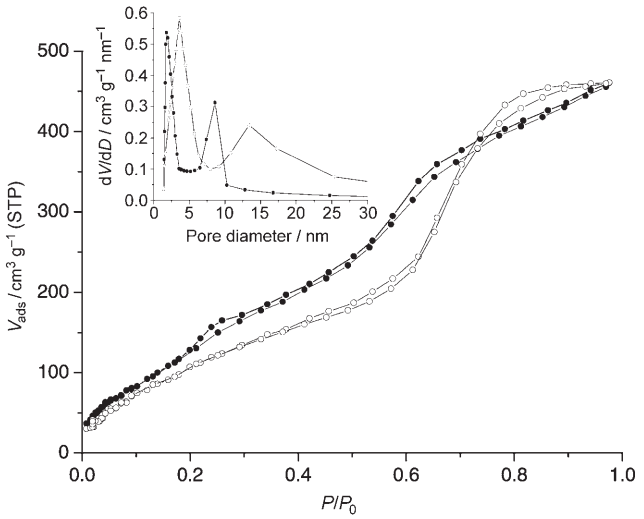

Figure 2. N_2 adsorption–desorption isotherms of the hierarchical mesoporous crystalline vanadium pentoxides synthesized with templates of CTAB/BMIC with the molar ratio 5:1 (○) and 1:1 (●). The corresponding Barret–Joyner–Halenda (BJH) pore-size distributions are shown in the inset.

of IL, which can effectively modify the leading CTAB-modeled structures (see above). Undoubtedly, the homogeneously narrow pore distribution endows this hierarchical multiporous vanadium pentoxide with more-pronounced material performance.

Figure 3 shows XRD patterns of the synthesized hierarchical multiporous materials. The stronger [001] and [110] peaks for CTAB/BMIC = 5:1 and [001] and [002] peaks for CTAB/BMIC = 1:1 indicate that the vanadium pentoxides are highly crystalline; this is consistent with the electron diffraction (ED) results. The growth orientation of mesoporous materials is dependent on the surface energy of various facets of the nuclei, whereas the hole channels of the template used determine the energy distribution to a large extent. Thus, the tunable ratios of CTAB/BMIC may easily model the growth dynamics of the nuclei of the vanadium

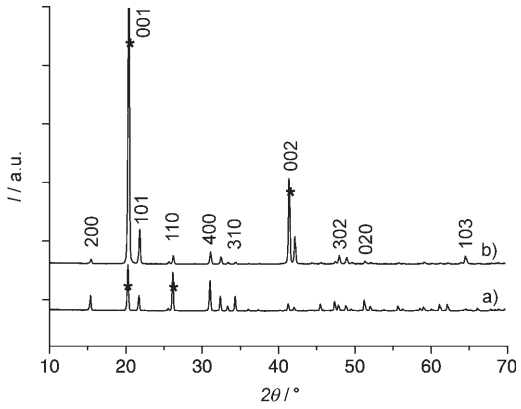

Figure 3. XRD spectra of the hierarchical mesoporous crystalline vanadium pentoxides synthesized with templates of CTAB/BMIC with the molar ratio a) 5:1 and b) 1:1.

species. The template-directed vanadium pentoxide with CTAB/BMIC = 1:1 shows much better crystallinity than that with CTAB/BMIC = 5:1, as the former displays only the sharp [001] peak of vanadium pentoxide. This multiporous vanadium pentoxide with a more orderly structure could serve as a much more promising functional material.

Figure 4 shows the thermal-decomposition behavior of the precursor of vanadium pentoxide, which provides direct in-

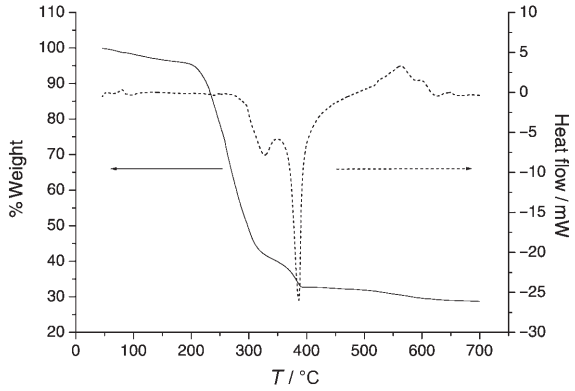

Figure 4. Thermogravimetric analysis (TGA; ——) and differential thermal analysis (DTA; -----) plots of the vanadium precursor in air from 20 to 700 °C at a rate of 10 °C min^{-1}.

formation about the transformation of vanadium from gel to final product under thermal treatment. The small initial weight loss of < 5 % under 200 °C was attributed mainly to the volatile solvent and surface-adsorbed free water; at this moment, the resultant sample was sensitive to water.[59] The following weight loss at 200–320 °C was due to the release of ammonia from ammonium metavanadate[60] from the partial decomposition of the cationic template CTAB.[61] An exothermal peak in the DTA curve in Figure 4 centered at 320 °C implies the breakup of the CTAB template structure. The further weight loss up to 395 °C was attributed to the removal of the cotemplate, and a corresponding sharp exothermal peak appeared at 395 °C in the DTA curve. These data show that the morphology of vanadium pentoxide controlled by the dual-template reagents disintegrated above 400 °C because of the complete decomposition of the templates. Although the nucleus formation and initial growth was attributed to the synergetic effect of the compatible dual templates used, it seems that the imidazolium-based IL is more beneficial to forming the 1D nanopores in terms of its internal imidazolium-directed rings. The special template behavior of ILs originate from the strong polarizability of the charged head group, thus leading to a stronger tendency for self-aggregation[58] and shrinking of the internal holes. When the temperature was increased to above 400 °C, there was no apparent weight loss. In this case, the vanadium pentoxide formed was well-crystallized as the temperature was elevated. The broad endothermal peak evident at about 560 °C provides support for the crystal-ordering process, which is endothermic.

Based on the above findings, the mechanism of formation of the crystalline vanadium pentoxide with hierarchical pores can be summarized briefly as follows. During the sol-gel process (Figure 5a–c), the long-chain cationic surfactant

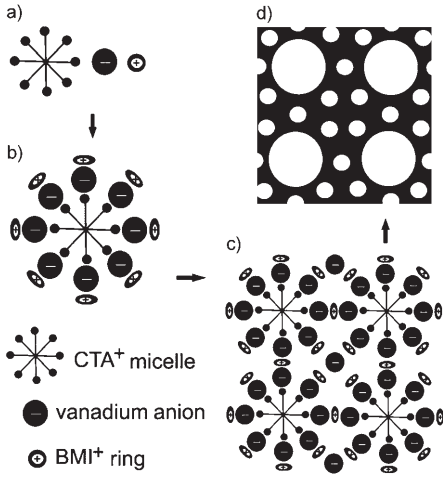

Figure 5. Schematic representation of the cotemplate process for the synthesis of hierarchical mesoporous crystalline vanadium pentoxide. a) Coexistence of CTA^+ micelle, $O(VO)O^-$, and BMI^+ ring; b) the self-assembled CTA^+–$O(VO)O^-$–BMI^+ entity; c) the orderly array network formed; d) the mesoporous framework after removal of the cotemplate.

CTAB automatically forms cationic micelles at a critical concentration. The head group CTA^+ combines with the vanadium anion $O(VO)O^-$ from the starting NH_4VO_3 source through electrostatic interaction.[62] Many 1D materials such as wires, whiskers, rods, and tubes have thus been successfully constructed by using a CTAB template.[63–66] However, the vanadium nucleus herein cannot grow outwards because of the effect of the BMI^+ ring, which is also attracted to the vanadium anion, at the other end. Therefore, a CTA^+–$O(VO)O^-$–BMI^+ entity is formed through electrostatic balance, in which the vanadium crystallite is effectively modeled by the cotemplate of suitable proportions. These randomly distributed CTA^+–$O(VO)O^-$–BMI^+ entities are further assembled thermodynamically during the ageing time, eventually building up an orderly array (Figure 5c). After removal of the dual templates by thermal treatment, the hierarchical mesoporous framework of the synthesized material is obtained (Figure 5d). It can be speculated from the framework that the larger mesopores are modeled basically from CTA^+ cationic micelles, whereas the smaller pores are mainly from the imidazolium rings of BMI^+. Due to the slightly lower decomposition temperature of CTAB than for BMIC (Figure 4), the larger mesopores formed from CTAB are more fragile and deform under the higher thermal stress. In other words, the imidazolium-based IL may play an important role in maintaining complete pore framework on account of its durable templating. This is also why the CTAB/BMIC = 1:1 modeled vanadium pentoxides have more shaped and complete pores than the 5:1 template products, owing to the more smaller mesopores from the former.

Previous reports[67,68] revealed that amorphous vanadium pentoxide exhibits apparent capacitive characteristics. However, crystalline vanadium pentoxide has not displayed any capacitive features so far. Herein the capacitive behavior of the synthesized crystalline vanadium pentoxides was initially explored in view of its orderly hierarchical multiporous properties. Figure 6 shows the cyclic voltammogram of the

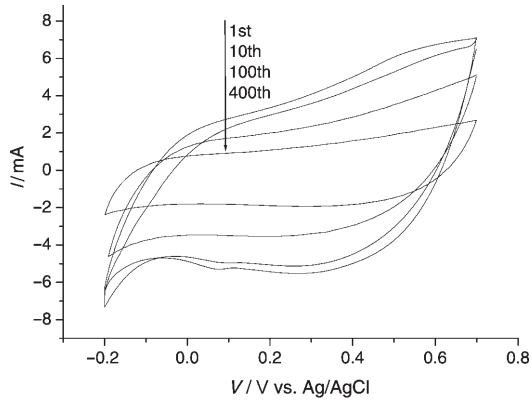

Figure 6. Cyclic voltammogram of the mesostructured crystalline vanadium pentoxide formed with the CTAB/BMIC = 1:1 cotemplate in KCl (2 M) at a scan rate of 10 $mV\,s^{-1}$.

crystalline vanadium pentoxides from the CTAB/BMIC = 1:1 cotemplate in a solution of KCl (2 M). Good capacitive behavior is demonstrated by the rounded curves. During the first few tens of cycles, a pair of small peaks on the anodic and cathodic sweeps that contribute pseudocapacitance with the insertion and extraction of active K^+ ions were observed. When the number of cycles was increased (typically to hundreds), the redox peaks disappeared, and at the same time the capacitance gradually declined. At the first cycle, the specific capacitance of synthesized crystalline vanadium pentoxide is 225 $F\,g^{-1}$. After 400 cycles, this value fell to 95 $F\,g^{-1}$. The disappearance of capacitance may be ascribed to structural changes due to stress from the insertion and extraction of K^+ ions, which can be verified with X-ray photoelectron spectroscopy (XPS).

Figure 7 shows the XPS profiles of the crystalline vanadium pentoxide before and after cyclic voltammetry measurements. The synthesized product is a typical orthorhombic V_2O_5 crystal. The bond energies of the V 2p and O 1s core levels are $E_B(V\ 2p_{3/2}) = 517.5$ eV, $E_B(V\ 2p_{1/2}) = 525$ eV and $E_B(O\ 1s) = 530.5$ eV, which agree with those reported in the literature.[69,70] After 400 cycles in KCl (2 M), the crystalline structure displays some evident changes. The small abnormal peaks at 524 and 533.5 eV represent vanadium oxides of low oxidation state and inactive potassium oxide. The spectrum was also fitted to reveal the components of the asymmetric peaks. It is clear that the V–O bond energy is not the same as that of the initial material, which means that a part of the vanadium pentoxide was reduced along with the insertion of K^+ ions. It can be assumed that vanadium oxides (i.e., V_2O_{5-n}) of low oxidation state damage the general

CHEMISTRY
AN ASIAN JOURNAL

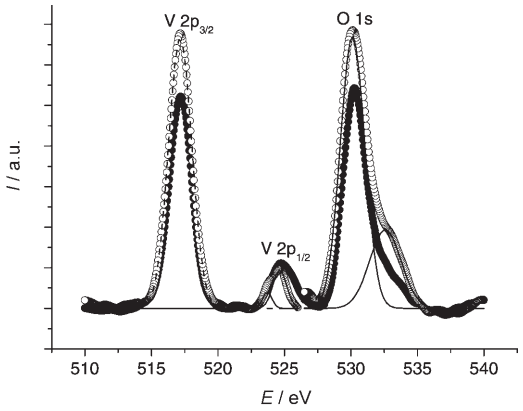

Figure 7. XPS spectra of the mesostructured crystalline vanadium pentoxide formed with the CTAB/BMIC = 1:1 cotemplate before (●) and after (○) 400 cycles in KCl (2 M) at a scan rate of 10 mV s.$^{-1}$ ——= Fit of the spectrum obtained after 400 cycles.

crystalline structure, thus blocking the transportation passage. On the other hand, the surplus oxygen vacancies may bind K^+ ions, which would lead to irreversible insertion. Two alternative solutions may be attempted to maintain capacitance. One is to dope a suitable stabilizer to keep the crystalline form; the disappearance of capacitance of MnO_2 was circumvented successfully by doping with Co to stabilize its form.[71] The other is the synthesis of vanadium composite materials including oxides of high oxidation state, which can effectively decrease the number of surplus oxygen vacancies.

Conclusions

We have successfully synthesized hierarchical mesoporous crystalline vanadium pentoxides by using a CTAB/BMIC cotemplate. The tunable ratios of CTAB to BMIC determine to a large extent the distribution and size of the hierarchical pores within this material. CTAB cationic surfactant contributes more to the larger mesopores, whereas BMIC ionic liquid is beneficial for forming the smaller pores. The vanadium-containing anions combine with CTA^+ micelles and BMI^+ rings through electrostatic forces. Thus, the growth orientation of the vanadium nucleus is modeled by the dual templates. The hierarchical mesoporous vanadium pentoxide directed by the cotemplate of CTAB/BMIC = 1:1 shows a more-orderly crystalline structure and demonstrates a large capacitance (225 F g^{-1}). However, due to continuous insertion/extraction of K^+ ions after hundreds of cycles, a structural change arises in the material, which results in the disappearance of capacitance. Measures could be taken for the preservation of capacitance in practical applications by doping with suitable structure stabilizers or by synthesizing stable vanadium composites.

Experimental Section

Synthesis

Ammonium metavanadate (0.002 mol, analytical grade; Shanghai) was soaked in solutions of pretreated ethanol (5 mL) containing different ratios of the template agents CTAB (analytical grade; Beijing) and BMIC (Fluka; washed twice with ethyl acetate before use). The mixtures were vigorously stirred for 36 h at room temperature, and pale-yellow homogeneous sols were obtained. The sols were allowed to age in air to form semitransparent gellike precursors, which were then transferred into a tube furnace and calcined in air. The temperature was raised to 650 °C at a rate of 20 °C min^{-1} and held there for 1 h. After annealing, the yellowish-brown products obtained were rinsed twice in sequence with absolute ethanol and double-deionized water to remove the remaining impurities.

Characterization

Field-emission SEM was performed on an XL30 ESEM FEG microscope at an accelerating voltage of 20 kV. TEM and ED were performed on a JEOL-JEM-2010 instrument at an accelerating voltage of 200 kV (JEOL, Japan). N_2 adsorption–desorption isotherms were determined on a Quantachrome NOVA 1000 (Version 6.11) system at 77 K. Specific surface areas were obtained by the BET method, and pore-size distribution was calculated from the adsorption branch of the isotherm by the BJH model. Powder XRD patterns were recorded on a PW1710 BASED X-ray diffractometer with $Cu_{K\alpha}$ radiation ($\lambda = 1.5406$ Å) at 40 kV and 30 mA. TGA and DTA were carried out with a Perkin–Elmer thermal-analysis TG/DTA system. The temperature was raised from 20 to 700 °C at a rate of 10 °C min^{-1} in air. XPS was conducted on a VG ESCALAB MK II spectrometer (VG Scientific, UK) with a monochromatic $Mg_{K\alpha}$ X-ray source ($h\nu = 1253.6$ eV). Peak positions were referenced internally to the C 1s peak at 284.6 eV.

Electrochemical measurements

The synthesized vanadium pentoxide powders, conducting graphite, acetylene black, and poly(vinylidene fluoride) (PVDF) binder were mixed in a weight ratio of 6.5:2:1:0.5 and carefully ground. The uniform mixtures were then rolled out on foam nickel and pressed at 2 MPa to form a slice that served as the working electrode. An Ag/AgCl electrode (with saturated KCl) and a clean Pt slice served as the reference and counter electrodes, respectively. A solution of KCl (2 M) was used as the electrolyte. This three-electrode system was connected to a CHI 630 electrochemical workstation to perform the cyclic voltammetric measurements.

Acknowledgements

We are thankful for the financial support provided by the National Natural Science Foundation of China (no. 20435010).

[1] C. T. Kresge, M. E. Leonowicz, W. J. Roth, J. C. Vartuli, J. S. Beck, *Nature* **1992**, *359*, 710.
[2] A. Imhof, D. J. Pine, *Nature* **1997**, *389*, 948.
[3] P. Yang, D. Zhao, D. I. Margolese, B. F. Chmelka, G. D. Stucky, *Nature* **1998**, *396*, 152.
[4] H. S. Yun, K. Miyazawa, H. Zhou, I. Honma, M. Kuwabara, *Adv. Mater.* **2001**, *13*, 1377.
[5] D. Grosso, G. J. A. A. Soler-Illia, F. Babonneau, C. Sanchez, P. A. Albouy, A. Brunet-Bruneau, A. R. Balkenende, *Adv. Mater.* **2001**, *13*, 1085.
[6] X. He, D. Antonelli, *Angew. Chem.* **2002**, *114*, 222; *Angew. Chem. Int. Ed.* **2002**, *41*, 214.
[7] X. Y. Kong, Z. L. Wang, *Nano Lett.* **2003**, *3*, 1625.
[8] S. Y. Choi, M. Mamak, N. Coombs, N. Chopra, G. A. Ozin, *Adv. Funct. Mater.* **2004**, *14*, 335.

[9] J.-G. Wang, M.-L. Tian, N. Kumar, T. E. Mallouk, *Nano Lett.* **2005**, 1247.
[10] W.-S. Chae, S.-W. Lee, Y.-R. Kim, *Chem. Mater.* **2005**, *17*, 3072.
[11] C. Ho, J. C. Yu, T. Kwong, A. C. Mak, S. Lai, *Chem. Mater.* **2005**, *17*, 4514.
[12] J. Roggenbuck, M. Tiemann, *J. Am. Chem. Soc.* **2005**, *127*, 1096.
[13] D. Zhao, J. Feng, Q. Huo, N. Melosh, G. H. Fredrickson, B. F. Chmelka, G. D. Stucky, *Science* **1998**, *279*, 548.
[14] D. Zhao, Q. Huo, J. Feng, B. F. Chmelka, G. D. Stucky, *J. Am. Chem. Soc.* **1998**, *120*, 6024.
[15] R. Ryoo, C. H. Ko, M. Kruk, V. Antochshuk, M. Jaroniec, *J. Phys. Chem. B* **2000**, *104*, 11465.
[16] T. Hyodo, Y. Shimizu, M. Egashira, *Electrochemistry* **2003**, *71*, 387.
[17] D. L. Lu, B. Lee, J. N. Kondo, K. Domen, *Microporous Mesoporous Mater.* **2004**, *75*, 203.
[18] Y. Y. Wu, G. S. Cheng, K. Katsov, S. W. Sides, J. F. Wang, J. Tang, G. H. Fredrickson, M. Moskovits, G. D. Stucky, *Nat. Mater.* **2004**, *3*, 816.
[19] Y. Zhou, M. Antonietti, *Adv. Mater.* **2003**, *15*, 1452.
[20] Y. Zhou, M. Antonietti, *Chem. Mater.* **2004**, *16*, 544.
[21] T. Brezesinski, C. Erpen, K. Iimura, B. Smarsly, *Chem. Mater.* **2005**, *17*, 1683.
[22] D. R. Rolison, *Science* **2003**, *299*, 1698.
[23] J. C. Yu, L. Z. Zhang, J. G. Yu, *New J. Chem.* **2002**, *26*, 416.
[24] Y. Shimizu, T. Hyodo, M. Egashira, *J. Eur. Ceram. Soc.* **2004**, *24*, 1389.
[25] A. K. Sinha, K. Suzuki, *J. Phys. Chem. B* **2005**, *109*, 1708.
[26] A. Corma, P. Atienzar, H. Garcia, J. Y. Chane-Ching, *Nat. Mater.* **2004**, *3*, 394.
[27] J. N. Kondo, M. Uchida, K. Nakajima, D. L. Lu, M. Hara, K. Domen, *Chem. Mater.* **2004**, *16*, 4304.
[28] Z. S. Chao, E. Ruckenstein, *Langmuir* **2002**, *18*, 8535.
[29] S. Ito, Y. Makari, T. Kitamura, Y. Wada, S. Yanagida, *J. Mater. Chem.* **2004**, *14*, 385.
[30] D. B. Lee, S. Passerini, A. L. Tipton, B. B. Owens, W. H. Smyrl, *J. Electrochem. Soc.* **1995**, *142*, L102.
[31] M. Garcia, S. H. Garofalini, *J. Electrochem. Soc.* **1999**, *146*, 840.
[32] P. E. Tang, J. S. Sakamoto, E. Baudrin, B. Dunn, *J. Non-Cryst. Solids* **2004**, *350*, 67.
[33] S. Nordlinder, J. Lindgren, T. Gustafsson, K. Edstrom, *J. Electrochem. Soc.* **2003**, *150*, E280.
[34] W. Li, S. H. Garofaliniz, *J. Electrochem. Soc.* **2005**, *152*, A364.
[35] C. Bolm, *Coord. Chem. Rev.* **2003**, *237*, 245.
[36] Y. Wang, Z. Liu, L. Zhan, Z. Huang, Q. Liu, J. Ma, *Chem. Eng. Sci.* **2004**, *59*, 5283.
[37] G. G. Janauer, A. Dobley, J. D. Guo, P. Zavalij, M. S. Whittingham, *Chem. Mater.* **1996**, *8*, 2096.
[38] P. Liu, S. H. Lee, C. E. Tracy, J. A. Turner, J. R. Pitts, S. K. Deb, *Solid State Ionics* **2003**, *165*, 223.
[39] T. Welton, *Chem. Rev.* **1999**, *99*, 2071.
[40] C. P. Mehnert, R. A. Cook, N. C. Dispenziere, E. J. Mozeleski, *Polyhedron* **2004**, *23*, 2679.
[41] B. C. Ranu, S. S. Dey, *Polyhedron* **2004**, *23*, 4183.
[42] S. J. Ding, M. Radosz, Y. Q. Shen, *Macromolecules* **2005**, *38*, 5921.
[43] Z. Li, H. Liu, Y. Liu, P. He, J. H. Li, *J. Phys. Chem. B* **2004**, *108*, 17512.
[44] H. Liu, P. He, Z. Li, Y. Liu, J. Li, L. Zheng, J. H. Li, *Electrochem. Solid-State Lett.* **2005**, *8*, J17.
[45] H. Liu, P. He, Z. Li, C. Sun, L. Shi, Y. Liu, G. Zhu, J. H. Li, *Electrochem. Commun.* **2005**, *7*, 1357.
[46] H. Liu, P. He, Z. Li, J. H. Li, *Nanotechnology* **2006**, *17*, 2167.
[47] P. He, H. Liu, Z. Li, J. H. Li, *J. Electrochem. Soc.* **2005**, *152*, E146.
[48] G. T. Wei, Z. S. Yang, J. C. Chen, *Anal. Chim. Acta* **2003**, *488*, 183.
[49] H. M. Luo, S. Dai, P. V. Bonnesen, *Anal. Chem.* **2004**, *76*, 2773.
[50] K. S. Khachatryan, S. V. Smirnova, I. I. Torocheshnikova, N. V. Shvedene, A. A. Formanovsky, I. V. Pletnev, *Anal. Bioanal. Chem.* **2005**, *381*, 464.
[51] S. Carda-Broch, A. Berthod, D. W. Armstrong, *Anal. Bioanal. Chem.* **2003**, *375*, 191.
[52] C. DeCastro, E. Sauvage, M. H. Valkenberg, W. F. Holderich, *J. Catal.* **2000**, *196*, 86.
[53] Y. Liu, M. Wang, Z. Li, H. Liu, P. He, J. H. Li, *Langmuir* **2005**, *21*, 1618.
[54] Y. Liu, M. Wang, J. Li, Z. Li, P. He, H. Liu, J. H. Li, *Chem. Commun.* **2005**, 1778.
[55] A. Lenourry, J. Gardiner, G. Stephens, *Biotechnol. Lett.*. **2005**, *27*, 161.
[56] Y. Zhou, J. H. Schattka, M. Antonietti, *Nano Lett.* **2004**, *4*, 477.
[57] K. Takahashi, S. J. Limmer, Y. Wang, G. Cao, *J. Phys. Chem. B* **2004**, *108*, 9795.
[58] M. Antonietti, D. B. Kuang, B. Smarsly, Z. Yong, *Angew. Chem.* **2004**, *116*, 5096; *Angew. Chem. Int. Ed.* **2004**, *43*, 4988.
[59] J. Wang, C. J. Curtis, D. L. Schulz, J.-G. Zhang, *J. Electrochem. Soc.* **2004**, *151*, A1.
[60] A. M. Kannan, A. Manthiram, *J. Electrochem. Soc.* **2003**, *150*, A990.
[61] Y.-D. Wang, C.-L. Ma, X.-D. Sun, H.-D. Li, *Mater. Lett.* **2001**, *51*, 285.
[62] Q. Huo, D. I. Margolese, U. Ciesla, P. Feng, T. E. Gier, P. Sieger, R. P. Leon, M. Petroff, F. Schuth, G. D. Stucky, *Nature* **1994**, *368*, 317.
[63] Y. Liu, D. Hou, G. Wang, *Chem. Phys. Lett.* **2003**, *379*, 67.
[64] M. Cao, C. Hu, Y. Wang, Y. Guo, C. Guo, E. Wang, *Chem. Commun.* **2003**, 1884.
[65] Y. Yu, F.-P. Du, J. C. Yu, Y.-Y. Zhuang, P.-K. Wong, *J. Solid State Chem.* **2004**, *177*, 4640.
[66] J. Perez-Juste, L. M. Liz-Marzan, S. Carnie, D. Y. C. Chan, P. Mulvaney, *Adv. Funct. Mater.* **2004**, *14*, 571.
[67] H. Y. Lee, J. B. Goodenough, *J. Solid State Chem.* **1999**, *148*, 84.
[68] T. Kudo, Y. Ikeda, T. Watanabe, M. Hibino, M. Miyayama, H. Abe, K. Kajita, *Solid State Ionics* **2002**, *152–153*, 833.
[69] Q.-H. Wu, A. Thißen, W. Jaegermann, *Solid State Ionics* **2004**, *167*, 155.
[70] J.-J. Shyue, M. R. De Guire, *Chem. Mater.* **2005**, *17*, 787.
[71] R. N. Reddy, R. G. Reddy, *J. Power Sources* **2004**, *132*, 315.

Received: May 31, 2006
Revised: August 11, 2006
Published online: October 13, 2006

